JCB Article

Calreticulin reveals a critical Ca^{2+} checkpoint in cardiac myofibrillogenesis

Jian Li,[1] Michel Pucéat,[2] Carmen Perez-Terzic,[2,4] Annabelle Mery,[2] Kimitoshi Nakamura,[3] Marek Michalak,[3] Karl-Heinz Krause,[1] and Marisa E. Jaconi[1]

[1]Biology of Aging Laboratory, Department of Geriatrics, Geneva University Hospitals, Geneva 1225, Switzerland
[2]CNRS UPR1086, Centre de Recherches de Biochime Macromoléculaire, Montpellier 34293, France
[3]CIHR Membrane Protein Research Group and Department of Biochemistry, University of Alberta, Edmonton T6G2H7, Canada
[4]Division of Cardiovascular Diseases, Deptartment of Medicine and Deptartment of Physical Medicine and Rehabilitation, Mayo Clinic, Mayo Foundation, Rochester, MN 55905

Calreticulin (*crt*) is an ubiquitously expressed and multifunctional Ca^{2+}-binding protein that regulates diverse vital cell functions, including Ca^{2+} storage in the ER and protein folding. Calreticulin deficiency in mice is lethal in utero due to defects in heart development and function. Herein, we used $crt^{-/-}$ embryonic stem (ES) cells differentiated in vitro into cardiac cells to investigate the molecular mechanisms underlying heart failure of knockout embryos. After 8 d of differentiation, beating areas were prominent in ES-derived wild-type (wt) embryoid bodies (EBs), but not in ES-derived $crt^{-/-}$ EBs, despite normal expression levels of cardiac transcription factors. $Crt^{-/-}$ EBs exhibited a severe decrease in expression and a lack of phosphorylation of ventricular myosin light chain 2 (MLC2v), resulting in an impaired organization of myofibrils. $Crt^{-/-}$ phenotype could be recreated in wt cells by chelating extracellular or cytoplasmic Ca^{2+} with EGTA or BAPTA, or by inhibiting Ca^{2+}/calmodulin-dependent kinases (CaMKs). An imposed ionomycin-triggered cystolic-free Ca^{2+} concentration ($[Ca^{2+}]_c$) elevation restored the expression, phosphorylation, and insertion of MLC2v into sarcomeric structures and in turn the myofibrillogenesis. The transcription factor myocyte enhancer factor C2 failed to accumulate into nuclei of $crt^{-/-}$ cardiac cells in the absence of ionomycin-triggered $[Ca^{2+}]_c$ increase. We conclude that the absence of calreticulin interferes with myofibril formation. Most importantly, calreticulin deficiency revealed the importance of a Ca^{2+}-dependent checkpoint critical for early events during cardiac myofibrillogenesis.

Introduction

Cardiogenesis is one of the earliest processes during vertebrate embryogenesis (Olson and Srivastava, 1996; Lin et al., 1997b; Black and Olson, 1998; Charron and Nemer, 1999; Harvey, 1999; Harvey and Rosental, 1999; Schwartz and Olson, 1999; Frey et al., 2000; Srivastava and Olson, 2000). Although intracellular Ca^{2+} is a critical second messenger in the heart, regulating diverse functions from gene expression to cell contraction and relaxation (Pozzan et al., 1994; Clapham, 1995), the potential contribution of Ca^{2+} signaling during early stages of cardiac development remains largely unexplored.

Within the ER, the Ca^{2+} reservoir of nonmuscle cells, Ca^{2+} is mainly bound to calreticulin (Michalak et al., 1999). Calreticulin is a highly conserved, 46-kD protein that modulates many cellular functions, including Ca^{2+} homeostasis (Liu et al., 1994; Bastianutto et al., 1995; Camacho and Lechleiter, 1995; Mery et al., 1996; Coppolino et al., 1997; Fasolato et al., 1998; John et al., 1998), protein folding (Helenius et al., 1997; Krause and Michalak, 1997; Ellgaard and Helenius, 2001), integrin-dependent cell adherence (Coppolino et al., 1995; Opas et al., 1996; Coppolino et al., 1997), and steroid-dependent gene expression (Burns et al., 1994; Dedhar et al., 1994).

Calreticulin is essential for proper cardiac development because knockout of the calreticulin gene is embryonically lethal due to impaired cardiac development (Mesaeli et al.,

Address correspondence to Marisa E. Jaconi, Laboratory of Biology of Ageing, Department of Geriatrics, Geneva University Hospitals, 2 Chemin du Petit Bel-Air, 1225 Chene-Bourg, Geneva 1225, Switzerland. Tel.: 41-22-305-5460. Fax: 41-22-305-5455.
E-mail: marisa.jaconi@medecine.unige.ch

C. Perez-Terzic's present address is Division of Cardiovascular Diseases, Department of Medicine and Department of Physical Medicine and Rehabilitation, Mayo Clinic, Mayo Foundation, Rochester, MN 55905.

K. Nakamura's present address is Department of Pediatrics, Kumamoto University, School of Medicine, Kumamoto 860-8556, Japan.

Key words: calreticulin; Ca^{2+}; embryonic stem cells; MEF2C; cardiac myofibrillogenesis

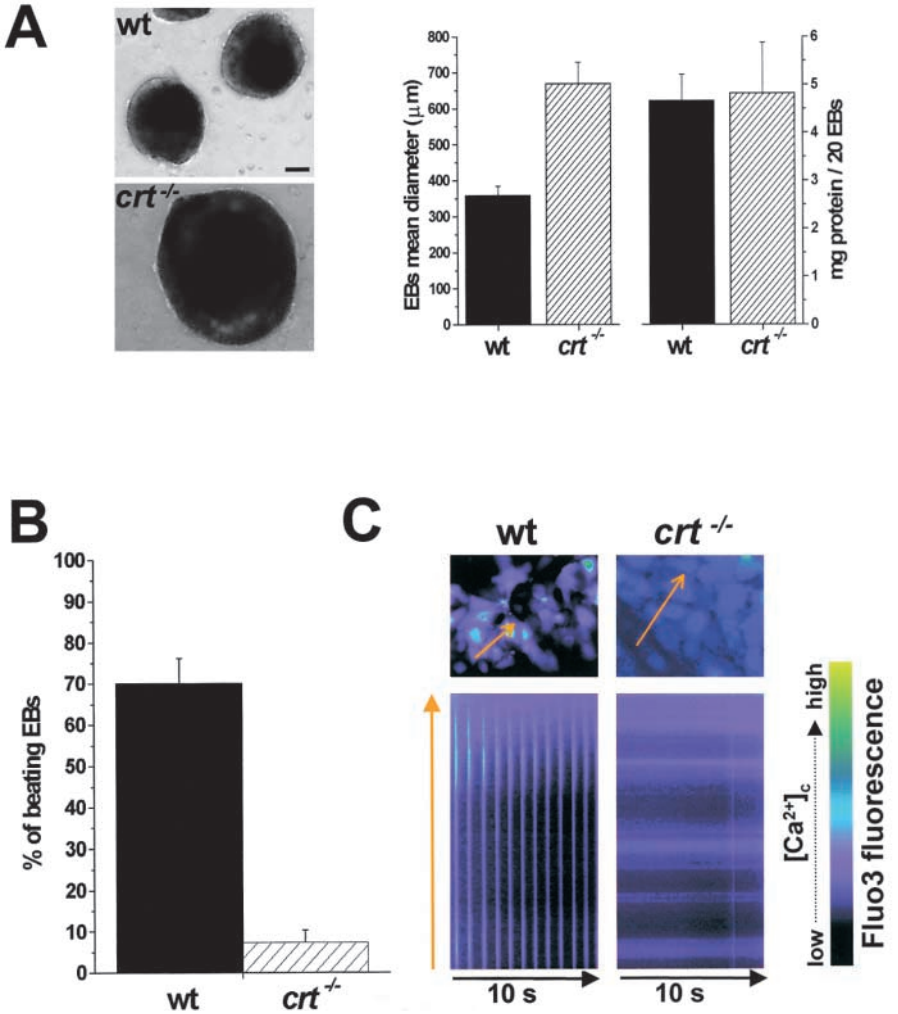

Figure 1. **Phenotype of wt or *crt*$^{-/-}$ embryoid bodies (EBs).** (A) (Left) Phase-contrast micrographs showing the macroscopic morphology of EBs derived from wt (top) or *crt*$^{-/-}$ (bottom) ES cells at D6 of culture. Bar, 100 μm. (Right) EB diameter and protein content of wt or *crt*$^{-/-}$ EB at D6 of culture. (B) Contractility: beating activity of EBs at D8 of culture. (C) Recording of oscillations in the $[Ca^{2+}]_c$ in wt (left) and *crt*$^{-/-}$ EBs (right). 8-d-old EBs were loaded with Fluo3 and $[Ca^{2+}]_c$ measured in a group of contracting cardiomyocytes. The line scan images represent changes in Fluo3 fluorescence along a line crossing a cardiomyocyte (arrows).

1999; Rauch et al., 2000). Calreticulin-null mouse embryos show a marked decrease in ventricular wall thickness and deep intertrabecular recesses in the ventricular walls (Mesaeli et al., 1999). Importantly, at early stages of cardiac development, calreticulin is highly expressed in differentiating cardiomyocytes (Mesaeli et al., 1999). It is subsequently downregulated in the mature heart (Mesaeli et al., 1999) because elevated expression of calreticulin in newborn hearts of transgenic mice leads to complete heart block and sudden death (Nakamura et al., 2001a).

Mechanisms responsible for impaired cardiac development in calreticulin-deficient (*crt*$^{-/-}$) mice are not well understood. Here we used calreticulin-deficient *crt*$^{-/-}$ embryonic stem (ES)* cells to investigate the role of the protein in early events of cardiac differentiation.

We show that calreticulin-deficient cardiomyocytes derived from ES cells had an impaired myofibrillogenesis due to decreased ventricular myosin light chain 2 (MLC2v) expression and phosphorylation. Nuclear translocation of myocyte enhancer factor C2 (MEF2C), a transcription factor responsible for activation of several cardiac specific embryonic genes, including the MLC2v, was inhibited in *crt*$^{-/-}$ cardiomyocytes. Furthermore, calreticulin-deficient myocytes featured disorganized myofilaments and inhibited contractile activity. Most importantly, this phenotype was reversed by transient elevation of cystolic-free calcium ($[Ca^{2+}]_c$) with a Ca^{2+} ionophore. This reveals a Ca^{2+}-dependent checkpoint in early events associated with cardiac myofibrillogenesis.

Results

Phenotype of calreticulin-deficient embryoid bodies

Fig. 1 shows that *crt*$^{-/-}$ embryoid bodies (EBs) cultured in suspension between day 2 (D2) and D6 had a significantly larger size than wild-type (wt) EBs (669 ± 60 μm, vs. 359 ± 26 μm, respectively), as measured at D6 (Fig. 1 A, left). Despite the size difference, both cell types had similar protein content as measured for 20 pooled EBs (4.66 ± 0.55 and 4.82 ± 1.06 μg/μl in wt and *crt*$^{-/-}$ EBs, respectively; $n = 3$; Fig. 1 A, right). In addition, no difference in the growing capacity (mitotic rate) of cultured wt versus *crt*$^{-/-}$ undifferentiated ES cells was observed (unpublished data).

Removal of leukemia inhibitory factor (LIF) from the culture medium induces ES cell differentiation (Maltsev et al.,

*Abbreviations used in this paper: $[Ca^{2+}]_c$, cystolic-free Ca^{2+} concentration; CaMK, Ca^{2+}/calmodulin-dependent kinase; *crt*, calreticulin; EB, embryoid body; ES, embryonic stem; LIF, leukemia inhibitory factor; MEF, mouse embryonic fibroblast; MEF2C, myocyte enhancer factor C2; MLC2a, atrial myosin light chain 2; MLC2v, ventricular myosin light chain 2; MLCK, myosin light chain kinase; wt, wild-type.

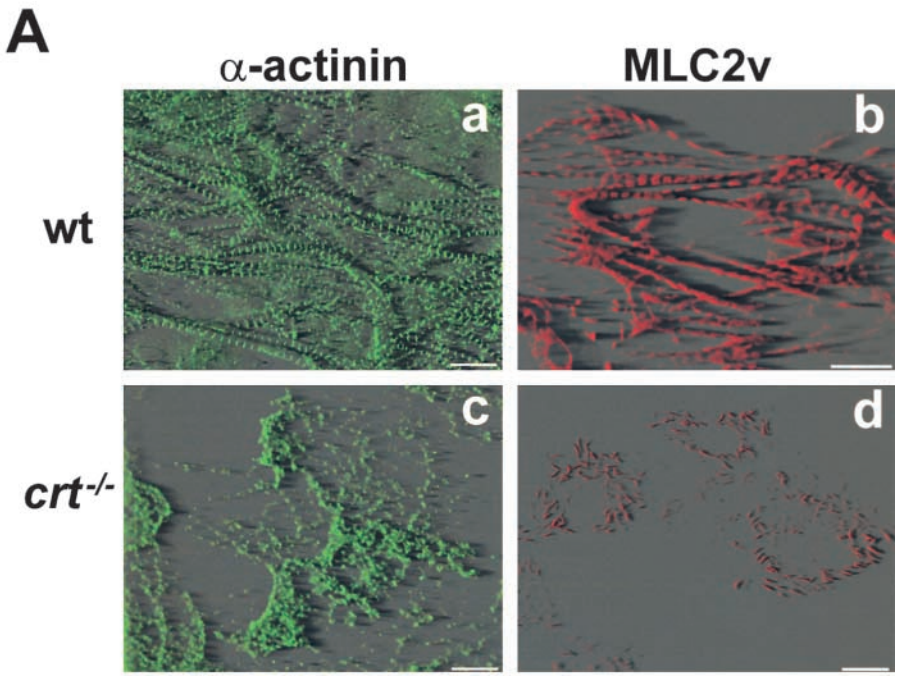

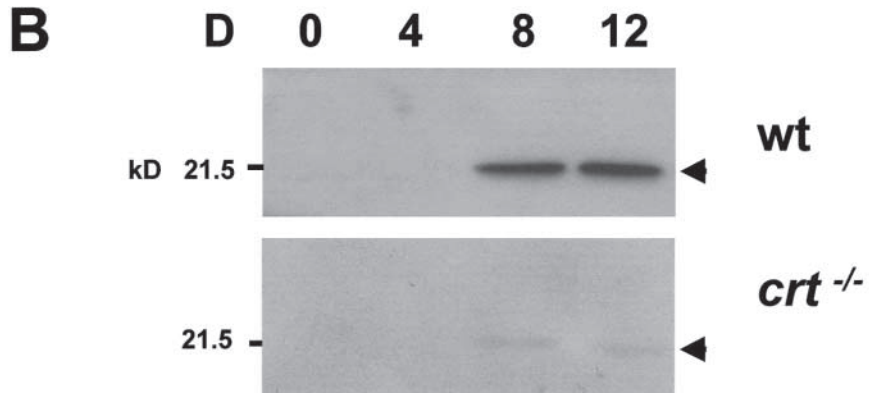

Figure 2. **Myofibrillogenesis in cardiomyocytes within EBs at D8 of differentiation.** (A) Distribution of α-actinin and MLC2v in control (a and b) and $crt^{-/-}$ cardiomyocytes (c and d). Proteins were visualized by staining with a mouse monoclonal anti–α-actinin antibody and a rabbit anti-MLC2v antiserum followed by a secondary anti–mouse FITC- or anti–rabbit Rhodamine-conjugated IgG, respectively. Each image was analyzed by digital deconvolution of 25–35 successive optical Z-sections (acquired with Metamorph software), and visualized as shadow projections of three-dimensional reconstructions (Imaris software). This figure is representative of five independent experiments. Bars, 10 μm. (B) MLC2v protein expression during the differentiation of wt or $crt^{-/-}$ EBs. Proteins extracted from EBs were separated by SDS-PAGE and transferred to a PDVF membrane. The blot was probed with a rabbit anti-MLC2v antiserum. The arrowheads indicate the location of MLC2v band.

1994) into EBs containing clusters of contracting cardioblasts after 7 d of culture (Meyer et al., 2000). Therefore, we analyzed for the presence of the contractile activity and the beating frequency of cardiomyocytes derived from wt and $crt^{-/-}$ ES cells at D8 of culture. Approximately 70% of the adherent wt EBs were strongly contracting and contained more than two beating areas, each beating with a frequency of 72 ± 8 contractions/min. In contrast, 90% of $crt^{-/-}$ EBs did not feature any contracting foci (Fig. 1 B). Wild-type EBs loaded with the Ca^{2+}-indicator dye fluo3 exhibited normal $[Ca^{2+}]_c$ oscillations (Fig. 1 C, left) (Bony et al., 2001), whereas $crt^{-/-}$ EBs did not show any measurable $[Ca^{2+}]_c$ spikes (Fig. 1 C, right).

The myofibrillogenesis was evaluated in 8-d-old EBs by in situ immunostaining of sarcomeric proteins α-actinin and MLC2v. As expected (Meyer et al., 2000), in wt ES-derived cardiomyocytes, α-actinin and MLC2v appeared organized as an interconnected network with the myofibrils stretching throughout the cytoplasm even by running from one cell into another (Fig. 2 A, a and b). These newly formed sarcomeres featured a length of 2 μm, similar to that of adult cardiac sarcomeres, indicating that the contractile apparatus was fully organized at this stage of EBs development. In contrast, $crt^{-/-}$ cardiomyocytes showed an anomalous distribution of both α-actinin and MLC2v (Fig. 2 A, c and d). α-actinin was not incorporated into the Z-disks but remained localized in cytosolic spots. MLC2v also failed to form and localize to the A bands. It was distributed within the cytosol as short disorganized filaments. In addition, a severe reduction in MLC2v mRNA and protein was also observed as revealed by reverse transcription–PCR (unpublished data) and Western blot analysis (Fig. 2 B), respectively. This indicated that calreticulin deficiency interferes with myofibril formation.

Effect of extracellular Ca^{2+} chelation, intracellular $[Ca^{2+}]_c$ buffering, and inhibition of calmodulin-dependent protein kinases on ES cell differentiation

Calreticulin-deficient mouse embryonic fibroblasts (MEFs) have impaired Ca^{2+} release from ER (Nakamura et al., 2001b). To test whether an altered Ca^{2+} homeostasis in cal-

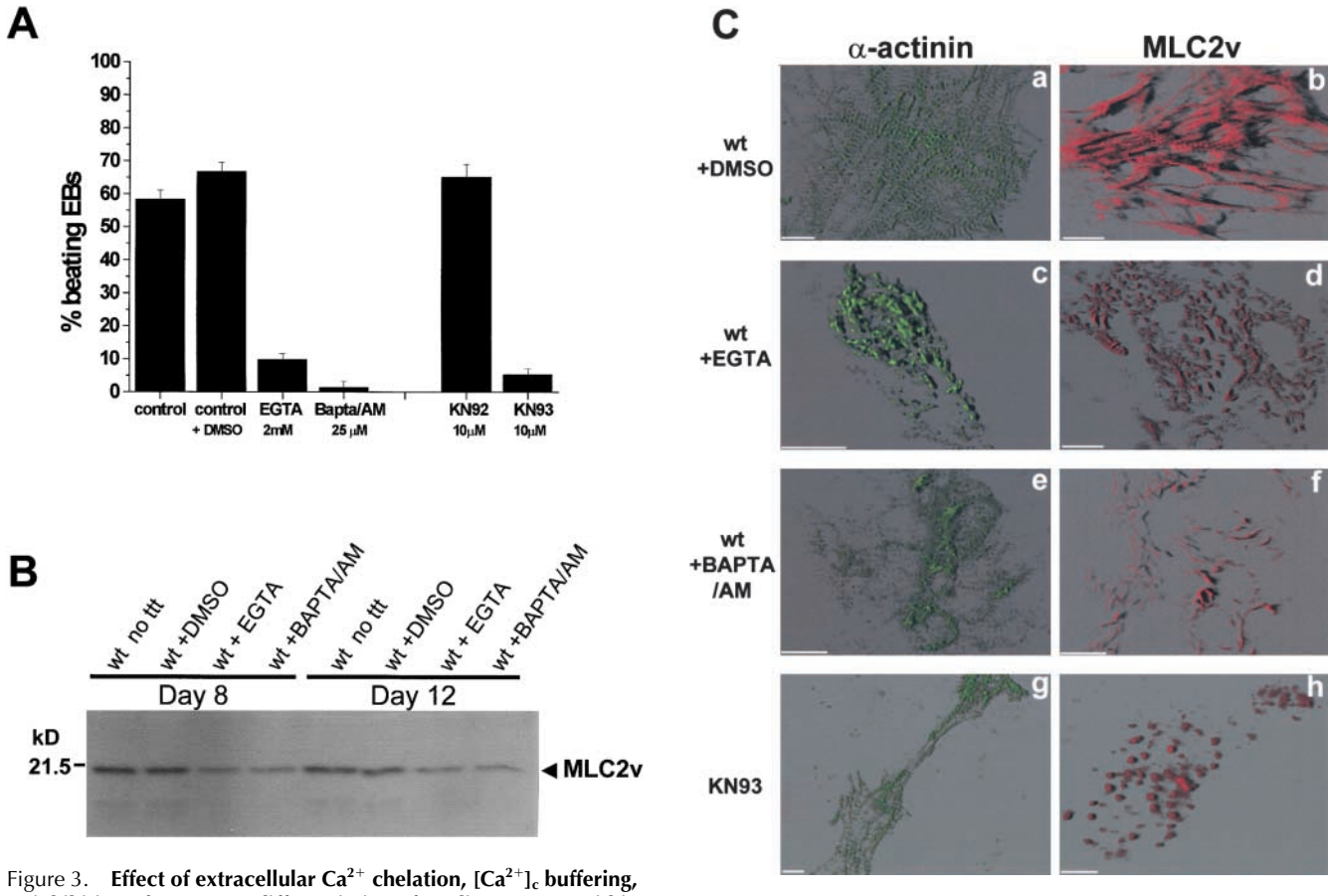

Figure 3. **Effect of extracellular Ca^{2+} chelation, $[Ca^{2+}]_c$ buffering, or inhibition of CaMKs on differentiation of cardiomyocytes within EBs.** (A) The presence of contracting foci within EBs at D8 of culture was evaluated after daily treatment of wt EBs starting at D4 of culture with: (1) untreated EBs; (2) DMSO (control solvent used for BAPTA and KN93); (3) 2 mM EGTA to buffer extracellular Ca^{2+}; (4) 25 μM BAPTA/AM to buffer $[Ca^{2+}]_c$; (5) 10 μM KN92; and (6) 10 μM KN93. (B) Effect of Ca^{2+} chelation and/or buffering protocols on the MLC2v expression in wt or *crt*$^{-/-}$ EBs, as analyzed by Western blot with the anti-MLC2v antiserum (IH treatment). (C) Immunolocalization of α-actinin (left) and MLC2v (rights) in EGTA- (2 mM) or BAPTA/AM-treated cells (25 μM). Shadow projections of three-dimensional reconstructions were generated as described in Fig. 2. Bars, 10 μm.

reticulin-deficient cardiomyocytes was responsible for an abnormal myofibrillogenesis and impaired contractility, we modulated extracellular or intracellular $[Ca^{2+}]_c$. Starting at D4 of differentiation, we either removed extracellular Ca^{2+} from the medium with EGTA (2 mM) or chelated $[Ca^{2+}]_c$ with BAPTA/AM (25 μM) during differentiation of wt EBs. D4 was chosen because at this time, although cardiac transcription factors are fully detectable by reverse transcription–PCR, no genes encoding constitutive cardiac proteins are yet expressed. Removal of extracellular Ca^{2+} or chelation of $[Ca^{2+}]_c$ led to a dramatic reduction in beating wt EBs observed at D8 (Fig. 3 A), and impaired myofibrillogenesis reminiscent of the calreticulin-deficient phenotype of EBs (Fig 2). Concomitantly, there was a reduction of MLC2v protein (Fig. 3 B).

The activation of Ca^{2+}/calmodulin-dependent protein kinases (CaMKs) is essential for myofibrillogenesis (Zhang et al., 2002) and sarcomere organization (Aoki et al., 2000). To test the involvement of CaMKs in EGTA or BAPTA-dependent inhibition of myofibrillogenesis we used KN93, an inhibitor of CaMKII (Sumi et al., 1991). wt EBs treated with KN93 from D4 to D8 had impaired distribution of both α-actinin and MLC2v, similar to the EGTA- or BAPTA-treated cells. Most importantly, they exhibited a phenotype similar to *crt*$^{-/-}$ cardiomyocytes. MLC2v was spread within the cytosol as short disorganized filaments (Fig. 3 C, d, f, and h vs. b for control), whereas α-actinin showed a spotted distribution (Fig. 3 C, c, e, and g). We concluded that elevation of $[Ca^{2+}]$ and activation of CaMK are essential for early stages of myofibrillogenesis, and that these processes are impaired in the absence of calreticulin.

Ca^{2+}-dependent rescue of the myofibrillogenesis in calreticulin-deficient cardiomyocytes

The phenotype of wt cells differentiated in the absence of extracellular Ca^{2+} or under Ca^{2+} buffering conditions was reminiscent of the phenotype of *crt*$^{-/-}$ cells. Therefore, we tested whether a transient elevation of $[Ca^{2+}]_c$ prior to myofibrillogenesis (i.e., appearance of recognizable cardiac cells) would initiate myofibril formation and restore the beating activity in the calreticulin-deficient EBs.

To elicit a transient increase in $[Ca^{2+}]_c$, we incubated *crt*$^{-/-}$ EBs at D4 with the Ca^{2+} ionophore ionomycin (10–1,000 nM) for 2 h, as indicated in Fig. 4 A. Only a 2-h treatment (followed by a washout) was used to exclude any potential toxic effect of ionomycin. Western blot analysis revealed no

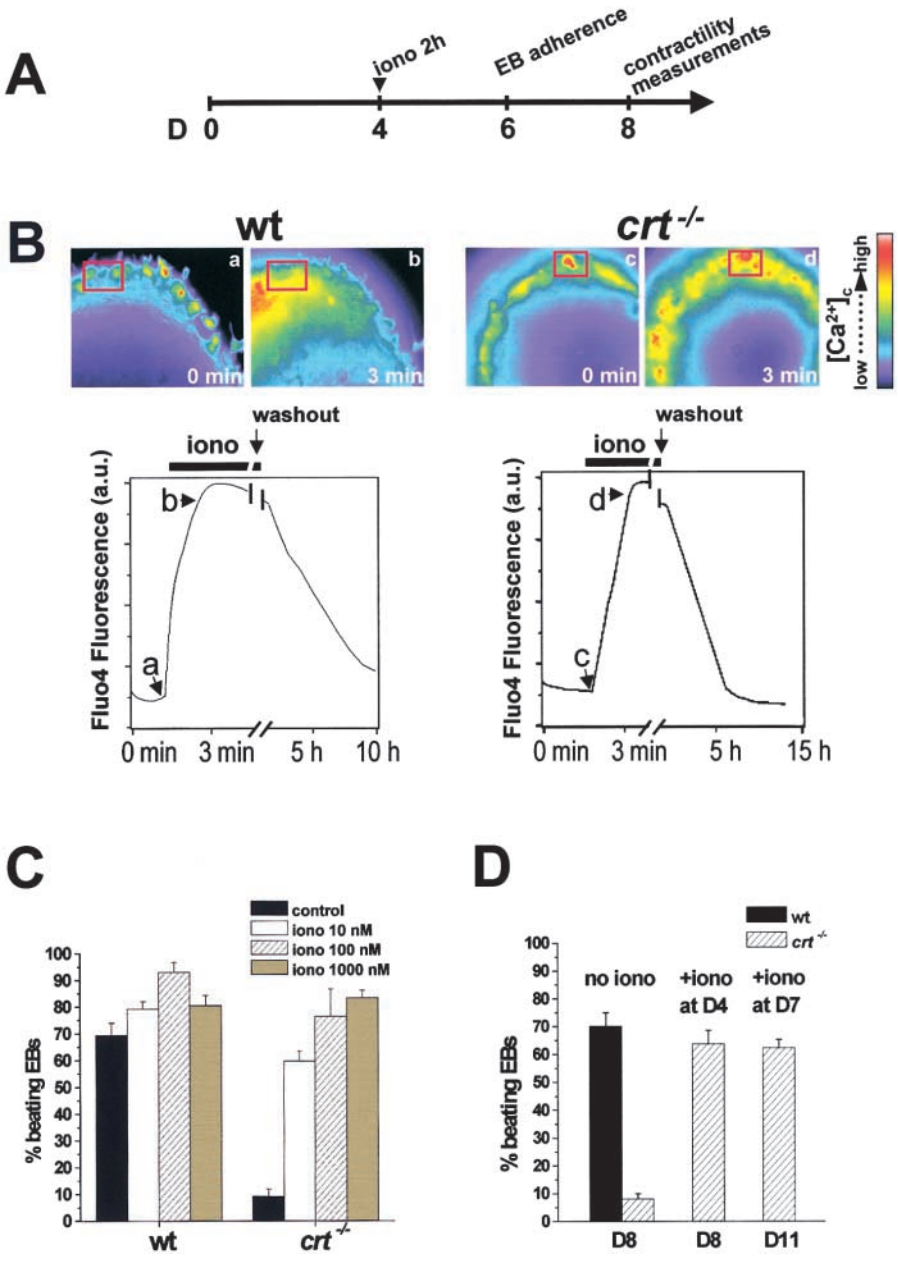

Figure 4. **Rescue of the contractile ability and the myofibrillogenesis in *crt*$^{-/-}$ cells by Ca^{2+} ionophore.** (A) Protocol of ionomycin treatment of EBs in the course of differentiation. (B) Effect of ionomycin on intracellular Ca^{2+} of fluo4-loaded wt or *crt*$^{-/-}$ EBs at D4. Fluo4-loaded EBs were cultured in a miniculture chamber on the stage of the microscope and challenged with 100 nM ionomycin for 2 h. After fluo4 reloading, ionomycin was washed out and Ca^{2+} measured for 10–15 h using the time-lapse mode of Metamorph (one measurement/30 min). (C) Dose–response increase of the contractile activity in *crt*$^{-/-}$ EBs treated with different concentrations of ionomycin. (D) Effect of 2 h treatment with ionomycin applied at D4 or D7 on beating activity of *crt*$^{-/-}$ EBs measured at D8, or D11, respectively.

significant change in the level of GRP94, a heat-shock ER chaperone of the HSP90 family normally upregulated after prolonged exposure to increased intracellular Ca^{2+} (Mitani et al., 1996) (unpublished data). This confirmed that this exposure of *crt*$^{-/-}$ cells to Ca^{2+} ionophore did not induce notable cell stress. Furthermore, we did not detect any cell death after ionomycin treatment, as determined by cell viability using trypan blue exclusion (3.8 ± 0.2% positive cells in control EBs vs. 3.4 ± 0.3% in ionomycin-treated EBs) and by extracellular release of cytosolic lactate dehydrogenase (1.5 ± 0.1% from control EBs vs. 2.0 ± 0.2% from ionomycin-treated EBs; $n = 3$).

Fig. 4 B shows that addition of 100 nM ionomycin to wt and *crt*$^{-/-}$ EBs induced a transient elevation in $[Ca^{2+}]_c$ in both types of EBs. After washout, $[Ca^{2+}]$ returned to basal level within 5 h.

Crt$^{-/-}$ ES-derived EBs were incubated with 10–100 nM ionomycin, at D4 (Fig. 4, C and D) or D7 (Fig. 4 D), followed by washout and analysis of their beating activity 4 d after addition of the ionophore. Fig. 4 C shows that *crt*$^{-/-}$ EBs treated with ionomycin had fully restored beating activity as rapidly as 4 d after ionomycin treatment. Partial recovery of EBs (20% beating EBs) was already observed the first day after incubation with ionomycin (unpublished data).

Next, we tested MLC2v expression in *crt*$^{-/-}$ cardiomyocytes within ionomycin-treated EBs. There was a correct insertion of both α-actinin and MLC2v into sarcomeric structures (Fig. 5 A), indicating that myofibrillogenesis was restored in *crt*$^{-/-}$ cells as a result of ionomycin treatment. Importantly, *crt*$^{-/-}$ EBs treated with ionomycin expressed high levels of MLC2v protein as observed for wt (Fig. 5 B).

Phosphorylation of MLC2v by the Ca^{2+}/calmodulin-dependent myosin light chain kinase (MLCK) is a prerequisite for its insertion into the A-band of the sarcomere (Sanbe et al., 1999). The phosphorylated and unphosphorylated forms of MLC2v can be readily identified by two-dimensional gel electrophoresis and followed by Western blot

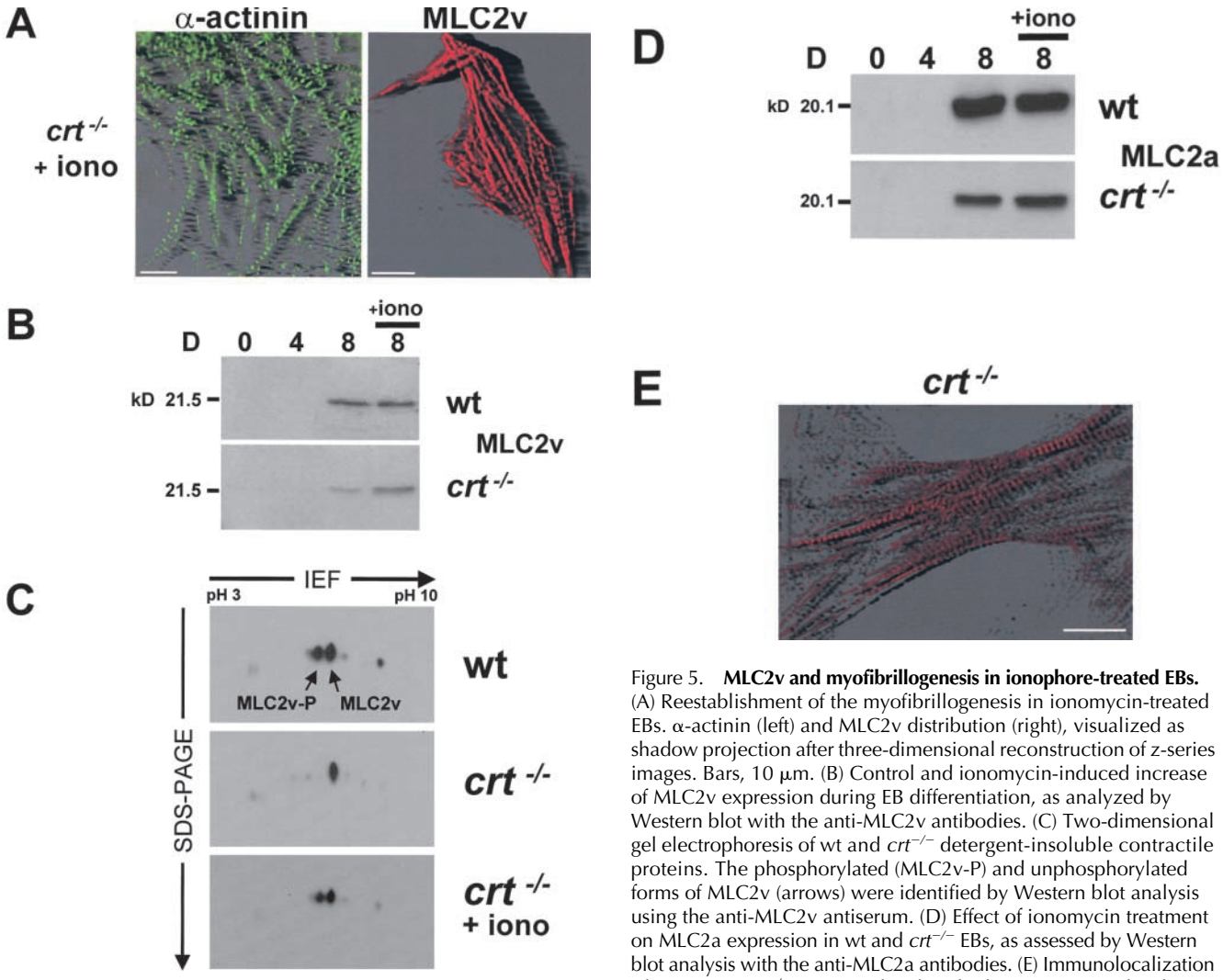

Figure 5. **MLC2v and myofibrillogenesis in ionophore-treated EBs.** (A) Reestablishment of the myofibrillogenesis in ionomycin-treated EBs. α-actinin (left) and MLC2v distribution (right), visualized as shadow projection after three-dimensional reconstruction of z-series images. Bars, 10 μm. (B) Control and ionomycin-induced increase of MLC2v expression during EB differentiation, as analyzed by Western blot with the anti-MLC2v antibodies. (C) Two-dimensional gel electrophoresis of wt and $crt^{-/-}$ detergent-insoluble contractile proteins. The phosphorylated (MLC2v-P) and unphosphorylated forms of MLC2v (arrows) were identified by Western blot analysis using the anti-MLC2v antiserum. (D) Effect of ionomycin treatment on MLC2a expression in wt and $crt^{-/-}$ EBs, as assessed by Western blot analysis with the anti-MLC2a antibodies. (E) Immunolocalization of MLC2a in $crt^{-/-}$ EBs, visualized as shadow projection after three-dimensional reconstruction of z-series images. Bar, 10 μm.

analysis with specific antibodies. As expected, wt EBs contained both phosphorylated and unphosphorylated forms of MLC2v. In contrast, in $crt^{-/-}$ cardiomyocytes, there was no detectable phosphorylated MLC2v (Fig. 5 C, middle). Most importantly, treatment of $crt^{-/-}$ EBs with ionomycin resulted in appearance of phosphorylated MLC2v (Fig. 5 C, bottom). This indicated that $crt^{-/-}$ cardiomyocytes feature impaired Ca^{2+}-dependent phosphorylation of MLC2v.

Interestingly, the content of atrial MLC2 (MLC2a) was not significantly affected by treating wt or $crt^{-/-}$ EBs with ionomycin (Fig. 5 D), and it was correctly inserted into sarcomeres in $crt^{-/-}$ cardiomyocytes (Fig. 5 E). We concluded that $crt^{-/-}$ EBs are deficient in a specific Ca^{2+} signal ("checkpoint") required for elevated expression of MLC2v (but not MLC2a), its phosphorylation, and assembly into functional sarcomeres.

Nuclear translocation of MEF2C is impaired in calreticulin-deficient cardiomyocytes

To investigate mechanisms responsible for downregulation of MLC2v in the absence of calreticulin, we measured expression and nuclear targeting of MEF2C, GATA4, and Nkx2.5, a group of cardiac transcription factors known to regulate the MLC2v gene expression. MEF2C, GATA4, and Nkx2.5 are detected as early as D4 to D5 of EB culture (Meyer et al., 2000). Real-time quantitative PCR analysis revealed no differences in the expression of all three transcription factors at D8 in wt and $crt^{-/-}$ EBs (Fig. 6 A). Ionomycin treatment had no significant effect on expression of MEF2C, GATA4, and Nkx2.5 in wt cells (Fig. 6 A); however, Western blot analysis revealed an increase in MEF2C levels in ionomycin-treated $crt^{-/-}$ EBs (Fig. 6 B). In contrast, GATA4 and NKx2.5 mRNA were decreased to 40 and 50%, respectively, in ionomycin-treated $crt^{-/-}$ EBs (Fig. 6 A). The increased level of MEF2C in ionomycin-treated cells was observed at the protein level in both wt and $crt^{-/-}$ EBs, whereas we did not detect any significant difference of MEF2C content in wt versus $crt^{-/-}$ under control conditions (Fig. 6 B).

Next, we investigated the localization of MEF2C, which regulates the activity of MLC2v promoter (Zou and Chien, 1995). Fig. 7 illustrates the intranuclear distribution of MEF2C within EBs. Distribution of nuclei within EBs was identified by Hoechst staining (Fig. 7, inset). In wt EBs, nuclei were strongly stained by the anti-MEF2C antibody, as visualized by the intranuclear three-dimensional distribution of MEF2C using the shadow projection mode (Fig. 7 A, a), as

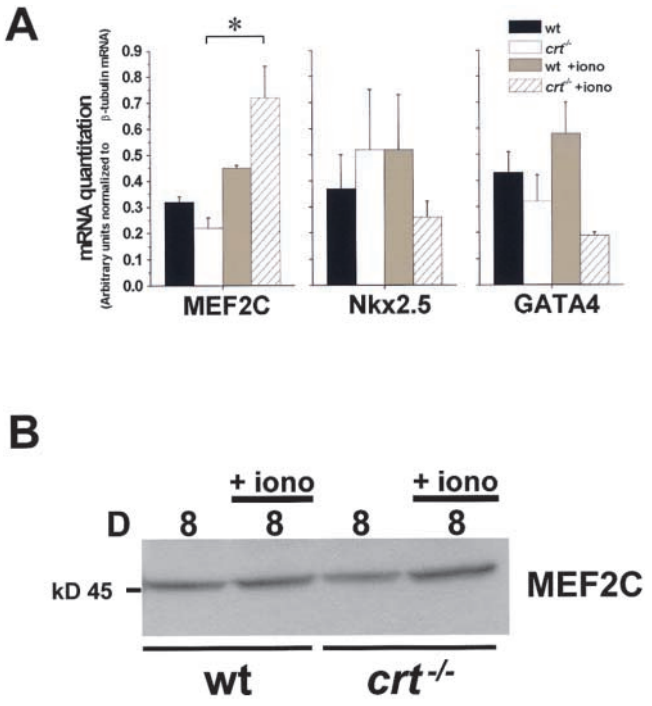

Figure 6. **Messenger RNA content and protein content of cardiac transcription factors in EBs.** (A) Effect of ionomycin treatment on the mRNA level of MEF2C, Nkx2.5, and GATA4 during the EB differentiation. EBs were incubated at D4 followed by RNA isolation at D8. Levels of mRNA were measured using real-time quantitative PCR *, $P < 0.001$. (B) Comparison of MEF2C protein expression in wt and $crt^{-/-}$ EBs during cardiac cell differentiation, as assessed by Western blot analysis with the anti-MEF2C antibodies.

well as by the summed fluorescence across the nuclei (Fig. 7 A, a′). In contrast, MEF2C failed to accumulate within the nuclei of $crt^{-/-}$ EBs and remained perinuclear (Fig. 7 A, b–b′). Importantly, the ionomycin-induced $[Ca^{2+}]_c$ elevation resulted in the restoration of MEF2C translocation into nuclei of $crt^{-/-}$ EBs (Fig. 7 A, d–d′), as well as in an increased accumulation of MEF2C into nuclei of wt cells (Fig. 7 A, c–c′). The impaired nuclear transport was specific to MEF2C because the intracellular distribution of another cardiac transcription factor, GATA4, was not affected. Fig. 7 C shows that GATA4 was localized to the nuclei in both wt and $crt^{-/-}$ cells, indicating that the nuclear import of this transcription factor was not affected by the absence of calreticulin. This indicates that Ca^{2+}-dependent processes are involved in the specific translocation of MEF2C to the nucleus of wt and $crt^{-/-}$ cells.

Next, we tested for a role of CaMKs in nuclear translocation of MEF2C. wt EBs were treated with KN93 from D4 to D8 to inhibit CaMK. In KN93-treated EBs, MEF2C was not targeted into the nucleus, resulting in the absence of contractile foci in these 8-d-old EBs (unpublished data; Fig. 3 A). KN92 was used as a negative control, and as expected, it did not affect MEF2C nuclear targeting or EB contractility.

Discussion

The generation of mice deficient in calreticulin has uncovered a critical role of the ER Ca^{2+}-binding protein (Mesaeli et al., 1999). Calreticulin-deficient mice display defects in heart development and function due to reduced thickness of the ventricular wall and impaired trabeculation (Mesaeli et al., 1999). Here we used calreticulin-deficient ES cells to investigate the molecular mechanisms responsible for the heart failure of $crt^{-/-}$ mice. We demonstrated that during the differentiation process, $crt^{-/-}$ ES-derived cardiomyocytes feature a severe disruption of myofibrillogenesis due to insufficient expression and Ca^{2+}-dependent phosphorylation of MLC2v. This is likely due to insufficient availability and mobilization of Ca^{2+} from ER in $crt^{-/-}$ cells as manifested by inhibited CaMK-dependent nuclear translocation of MEF2C. The importance of Ca^{2+} in these processes is documented by rescue of $crt^{-/-}$ phenotype with Ca^{2+} ionophore. We show that differentiation proceeds normally at the very early stages of $crt^{-/-}$ EBs formation, but that they fail to undergo normal myofibril formation in the absence of calreticulin and a specific ER-dependent Ca^{2+} signal. We propose that a specific Ca^{2+}-dependent checkpoint is required for myofibrillogenesis. This signal is not generated in the absence of calreticulin.

Early cardiogenesis is regulated by three families of transcription factors (i.e., Nkx2.5, MEF2, GATA) (Srivastava and Olson, 2000). Among these factors, MEF2C is an essential regulator of ventricular development (Black and Olson, 1998). The targeted disruption of the MEF2C gene in the mouse results in embryonic lethality due to cardiac developmental arrest and severe downregulation of a number of cardiac markers (Durocher et al., 1996; Lin et al., 1997a; Charron and Nemer, 1999) including MLC2v (Liu et al., 2001). MEF2C is a major cardiac transcription factor regulating the activity of MLC2v promoter (Chen et al., 1998; Nguyen-Tran et al., 1999). Therefore, it is not surprising that impaired Ca^{2+}-dependent nuclear translocation of MEF2C in $crt^{-/-}$ cells results in low expression of MLC2v, and consequently impaired myofibrillogenesis.

MEF2 is at the crossroad of multiple $[Ca^{2+}]_c$ signals, which affect transcriptional processes (Olson and Srivastava, 1996). Here we show that MEF2C function depends on the presence of a calreticulin-dependent signal. MEF2 integrates Ca^{2+}-dependent signals involving calcineurin, CaMKI, CaMKIV, MKK6/p38 MAPK, and extracellular signal-regulated kinase 5 (Yang et al., 1998; Blaeser et al., 2000; Friday et al., 2000; Han and Molkentin, 2000; Passier et al., 2000). $Crt^{-/-}$ ES-derived cardiomyocytes have normal expression of MEF2C, GATA4, or Nkx2.5, but have an impaired nuclear translocation of MEF2C. MEF2C remains in the cytosol and in perinuclear area in $crt^{-/-}$ ES-derived cardiomyocytes, whereas it is inside the nucleus in wt cells. This is specific for MEF2C because nuclear localization of GATA4 is not affected in $crt^{-/-}$ cardiomyocytes. Indeed, GATA4 was correctly targeted to the nucleus of these cells. Therefore, our data do not favor the hypothesis that the absence of calreticulin, by affecting the Ca^{2+} filling state of the stores and the nuclear cisternae, could indiscriminately impair the nuclear import of transcription factors through a conformational closure of nuclear pores after an upward shift of the transporter (Perez-Terzic et al., 1996). How nuclear import of macromolecules including MEF2C is impaired in $crt^{-/-}$ cardiomyocytes is currently under investigation.

As expected, MLC2a expression is significantly less affected in $crt^{-/-}$ cardiomyocytes, as it is likely activated by GATA4 and

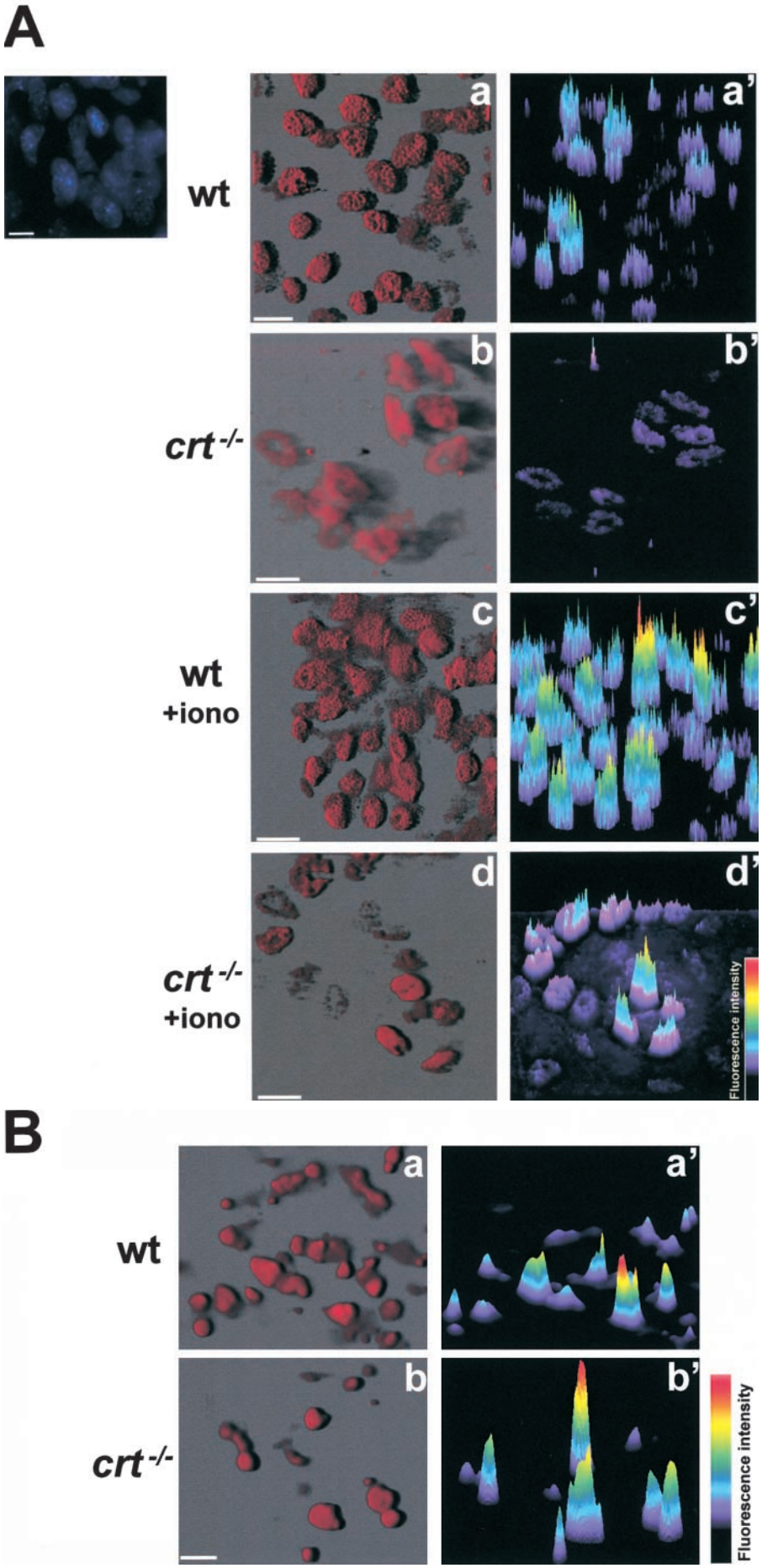

Figure 7. **Study of the intracellular localization of MEF2C in clustered cardiomyocytes within EBs.** (A) Three-dimensional representation of MEF2C immunolocalization in cardiomyocytes within EBs at D8 of differentiation. (a to d) Shadow projections. (a′ to d′) Profiles on the x–y dimension of MEF2C intranuclear localization visualized as the summed fluorescence distribution across the nuclei (fluorescence of middle plan crossing the nuclei in the z-axis). (a and a′ and c and c′) wt EBs ± ionomycin respectively. (b and b′ and d and d′) $crt^{-/-}$ EBs ± ionomycin. (a and b) wt and $crt^{-/-}$ cells EB, respectively, in control conditions (addition of DMSO). (c and d) wt and $crt^{-/-}$ cells treated with ionomycin, respectively. (Inset) Hoechst staining of nuclei within an EBs. (B) Profile on the x–y dimension of GATA4 intranuclear localization visualized as the summed fluorescence distribution across the nuclei (fluorescence of middle plan crossing the nuclei in the z-axis). Bars, 10 μm (100 nuclei analyzed in four different experiments).

Nkx2.5 factors (Gruber et al., 1998; Franco et al., 1999; Nguyen-Tran et al., 1999; Doevendans et al., 2000). The presence of correctly inserted MLC2a is likely to account for some contractility observed in 5–10% of $crt^{-/-}$ EBs. This is in line with calreticulin-knockout gene studies which showed that calreticulin deficiency primarily affects ventricular development and has no significant effect on atrial cells (Mesaeli et al., 1999).

Although inhibited nuclear translocation of MEF2C in $crt^{-/-}$ cardiomyocytes explains the reduced expression of MLC2v, it cannot account for the lack of insertion of the existing light chains into functional sarcomeres. We show that the latter defect is likely attributed to low active Ca^{2+}/calmodulin-dependent MLCK, which is required to phosphorylate MLC2v prior to its assembly into sarcomeric units and to ensure a normal Ca^{2+} sensitivity of myofilaments (Clement et al., 1992; Sanbe et al., 1999).

The most important finding of this study is that the calreticulin-deficient phenotype can be rescued by increasing $[Ca^{2+}]_c$ in $crt^{-/-}$ EBs. Treatment of EBs at D4 or D7 with ionomycin restores the CaMK-dependent intranuclear localization of MEF2C, MLC2v phosphorylation, its sarcomeric insertion and contractility in $crt^{-/-}$ EBs. In line with these observations, inhibition of CaMK with KN93, chelation of intracellular Ca^{2+} (BAPTA), or preventing Ca^{2+} influx in EGTA-buffered extracellular medium abolishes nuclear localization of MEF2C in wt EBs. Thus, phosphorylation of MEF2C by a cytosolic CaMK (Colomer and Means, 2000; Olson and Williams, 2000; Corcoran and Means, 2001), is required for its intranuclear targeting.

An elevation of $[Ca^{2+}]_c$ by either a Ca^{2+} influx across the plasma membrane and/or Ca^{2+} release from the ER is required to activate CaMKs, including MLCK to drive cardiac myofibrillogenesis. In early cardiomyocytes differentiated within EBs, the initiation of spontaneous contractions is triggered by inositol 1,4,5-trisphosphate–dependent $[Ca^{2+}]_c$ oscillations from the ER and it does not require Ca^{2+}-induced Ca^{2+} release from the sarcoplasmic reticulum (Viatchenko-Karpinski et al., 1999). $Crt^{-/-}$ cardiomyocytes do not feature any spontaneous $[Ca^{2+}]_c$ spikes, suggesting a defect in inositol 1,4,5-trisphosphate signaling in calreticulin-deficient cardiomyocytes. Although rapid $[Ca^{2+}]_c$ signals induce events such as muscle contraction, secretion, adhesion, and and synaptic transmission, more sustained $[Ca^{2+}]_c$ signals are known to be involved in cell proliferation and differentiation. We rescued the expression, the phosphorylation, and the assembly of MLC2v into sarcomeric units by triggering a transient but long-lasting $[Ca^{2+}]_c$ increase in $crt^{-/-}$ EBs before the appearance of contractions (i.e., D4 or D7) using the Ca^{2+} ionophore, ionomycin. This treatment led to a recovery of contractility in $crt^{-/-}$ ES-derived cardiomyocytes. Although applied for a brief period (2 h), ionomycin induced a transient but long-lasting Ca^{2+} influx into the embryoid body as previously shown in other cell types (Timmerman et al., 1996; Durham and Russo, 2000). This ionophore-dependent Ca^{2+} increase mimics receptor-mediated Ca^{2+} elevation into the cytosol, an event missing in $crt^{-/-}$ EBs. It further resets the cardiac differentiation program, paused after an early stage of cardiac commitment.

In summary, although $crt^{-/-}$ cells seem to undergo a normal cardiac commitment up to D4 (time of maximal expression of cardiac transcription factors) (Meyer et al., 2000), they have lost the ability to achieve the full differentiation program, waiting for a Ca^{2+} signal. This is similar to a Ca^{2+}-dependent block involving CaMKs activation as reported during the development of *Xenopus* eggs (Lorca et al., 1993). Thus, we provide evidence that a Ca^{2+}-dependent checkpoint involving $[Ca^{2+}]_c$ elevation in the cytoplasm and activation of CaMKs is required at an early stage of differentiation to allow cardiac precursors to fully differentiate into cardiomyocytes. This Ca^{2+} checkpoint plays a dual role: it modulates Ca^{2+}-dependent nuclear translocation of specific transcription factor, and it activates Ca^{2+}-dependent kinases (and phosphatases) involved in early cardiac myofibrillogenesis.

Materials and methods

Embryonic stem cell culture and differentiation

wt or $crt^{-/-}$ ES cells derived from J1 129/Sv mice were propagated on feeder cells (mitomycin-treated mouse embryonic fibroblasts) using BHK21 medium (GIBCO BRL) supplemented with pyruvate, nonessential amino acids, mercaptoethanol, glutamine, 10% fetal calf serum (Biomedia) (Smith, 1992), and LIF-conditioned medium, obtained from preconfluent 740 LIF-D cells, stably transfected with a plasmid encoding LIF (Meyer et al., 2000).

The cells were maintained at <70% confluency to keep an undifferentiated phenotype. ES cells were differentiated in vitro as embryo-like aggregates (EBs) using the hanging drop method (Maltsev et al., 1994). Briefly, EBs were formed for 2 d (D0–D2) in hanging drops (450 cells/20μl) of differentiation medium (BHK21, as described above), containing 20% fetal calf serum and lacking of LIF. The EBs were then incubated in suspension for 3 d (D2–D5) and transferred to gelatin-coated dishes or glass coverslips (at D6). The differentiating EBs were examined daily under phase-contrast microscopy for the presence of contracting cardiomyocytes.

Antibodies and immunocytochemistry

For immunostaining, EBs were fixed with 3% paraformaldehyde, permeabilized with 0.1% Triton X-100, and labeled with mouse monoclonal anti-MEF2C (1/50) (Cell Signaling), anti-α-actinin antibodies (1/500) (Sigma-Aldrich), with rabbit anti-MLC2v (1/50), or anti-MLC2a (1/500) antisera (Meyer et al., 2000). Secondary antibodies included rhodamine-conjugated goat anti–rabbit IgG and FITC-conjugated goat anti–mouse IgG (Sigma-Aldrich) (dilutions 1/100) (Jaconi et al., 2000). Cell nuclei were visualized within the EBs by Hoechst staining.

Imaging of cytosolic calcium levels

EBs adherent on glass coverslips were loaded at D 4 or D8 with 5 μM fluo3 or fluo4/AM (Molecular Probes) for 20 min, and transferred to the stage of an epifluorescence microscope and perfused with a medium containing 20 mM Hepes, 117 mM NaCl, 5.7 mM KCl, 1.2 mM NaH_2PO_4, 4.4 mM $NaHCO_3$, 1.7 mM $MgCl_2$, and 1.8 mM $CaCl_2$, pH 7.4. The field was illuminated at 485 ± 22 nm with a Xenon lamp. Fluo3 or fluo 4 emission fluorescence was recorded through a dichroic mirror (cutoff 510 nm) and a long pass emission filter (cutoff 520 nm) (Jaconi et al., 2000). The fluorescent images were recorded at 530 nm long pass filter, using a Nikon (diaphot) or Leica (DMRA) microscope coupled to a CCD camera (micromax 1300Y/HS; Princeton) and digitized on line by a computer (Metamorph software; Universal Imaging). To calculate the frequency of $[Ca^{2+}]_c$ spikes in embryoid bodies, a region of interest was selected within a beating area and the average pixel intensity was plotted as a function of time. To record long-term changes in $[Ca^{2+}]_c$ induced by ionomycin using time-lapse video microscopy (Metamorph software), EBs were loaded with fluo4 prior to ionomycin application and reloaded 2 h later after washout of the ionophore. EBs were also reloaded with fluo4 at the end of the time-lapse experiment to determine whether the low levels of Ca^{2+} were due to a leakage of the probe. EBs were illuminated for 2 s, and z-stacks of images were acquired every 15 min for up to 10 h.

All experiments were performed at 35 ± 2°C, under 95%O_2/5% CO_2 atmosphere, and have been repeated on three separate occasions.

Cell imaging

Images of the adherent EBs were acquired with a 12-bit, cooled charge-coupled device interlined camera (Visicam; Visitron System) mounted on a Nikon Eclipse epifluorescence microscope, equipped with 40×, 63×, 100×, 1.3 NA oil-immersion objectives. A monochromator coupled to an optic fiber (Delta-

Ram, Photon Technology International) allowed the excitation for the FITC (488 nm, DM505, BA 520–560 nm) and the rhodamine (545 nm, DM575, BA 590) fluorescence respectively. Optical z-sectioning (0.2-μm step) was achieved using an objective-mounted piezo-electric controller (LVPDZ position servo controller; Physik Instrumente) driven by the Metamorph 4.1 software (Visitron; Universal Imaging). The stack of images, stored as volume files, were processed by the software Huygens to perform digital restoration of the images (Huygens 2.2.1; Scientific Volume Imaging) and visualized after three-dimensional reconstruction using the Imaris software (Bitplane). All calculations were performed using an Octane workstation (Silicon Graphics).

RNA extraction and reverse transcription reaction

Total cellular RNA was isolated from EBs using the RNA Extraction Kit (Perfect RNA Mini Kit; Eppendorf). Residual genomic DNA was removed by incubating the RNA solution with 15 units of RNase-free DNase I (CLONTECH Laboratories, Inc.) in 2 mM $MgCl_2$ for 45 min at 37°C, followed by inactivation at 90°C for 5 min. 1 μg of DNase-treated RNA was reverse transcribed using the Superscript II kit (GIBCO BRL). The cDNA was diluted 10-fold prior to PCR amplification.

Real-Time quantitative PCR by SYBR green detection

The nucleotide sequences of the PCR primers used were: MEF2C forward 5′-AGATACCCACAACACACCACGCGCC and reverse 5′-ATCCTTCAGAGAGTCGCATGCGCTT; GATA4 forward 5′-CGAGATGGGACGGGACACT and reverse 5′-CTCACCCTCG-GCCATTACGA; and Nkx2.5 forward 5′-TGCAGAAGGCAGTGGAGCTGGACAAGCC and reverse 5′-TTGCACTTGTAGCGACGGTTCTGGAACCAG; β-tubulin forward 5′-CCGGACAGTGTGGCAACCAGATCGG and reverse 5′-TGGCCAAAAGGACCTGAGCGAACGG. Real-time quantitative PCR was performed using a LightCycler rapid thermal cycler (Roche). Amplification was carried out as recommended by the manufacturer. 12 μl reaction mixture contained 1 μl of LightCycler-DNA Master SYBR Green I mix (FAST Start KIT, containing Taq DNA polymerase, reaction buffer, deoxynucleoside trisphosphate mix, and SYBR Green I dye), 3 mM $MgCl_2$, and 0.5 μM concentration of appropriate primer and 2 μl of cDNA. The relative cDNA concentrations were established by a standard curve using sequential dilutions of corresponding PCR fragments. The data were normalized by PCR analysis of the β-tubulin. The amplification program included the initial denaturation step at 95°C for 8 min, and 40 cycles of denaturation at 95°C for 3–5 s, annealing at 60–65°C for 6–10 s, and extension at 72°C for 5–10 s. The temperature transition rate was 20°C/s. Fluorescence was measured at the end of each extension step. After amplification, a melting curve was acquired by heating the product at 20°C/s to 95°C, cooling it at 20°C/s to 70°C, keeping it at 70°C for 20 s, and then slowly heating it at 0.1°C/s to 95°C. Fluorescence was measured through the slow heating phase. Melting curves were used to determine the specificity of PCR products, which were further confirmed using conventional gel electrophoresis.

The Student's *t* test was used to analyze statistical significance. All p values corresponded to two-tailed tests, and a P of <0.05 was considered statistically significant.

Western blotting analyses

The MLC2v and MEF2C proteins were identified by Western blot analysis (Towbin et al., 1979; Clement et al., 1992). In brief, whole-cell lysate from 50 to 60 EBs was obtained using RIPA buffer (20 mM Tris-HCl, pH 7.8, 150 mM NaCl, 1% Triton X-100, 1% deoxycholic acid, 1mM EDTA, 0.05% SDS) supplemented with a protease inhibitors cocktail (Complete™ Mini; Boehringer Mannheim). Protein concentrations were determined by BioRad protein assay. Proteins (50–70 μg) were fractionated by SDS-PAGE, electroblotted onto PVDF Immobilon-P transfer membrane (Millipore), and probed with anti–MLC2v (dilution 1/500) or anti–MLC2a antisera (1/5,000), or with anti–MEF2C antibody (dilution 1/1,000). Antibodies were visualized by addition of HRP goat anti–rabbit IgG and enhanced chemiluminescence reagents (ECL reagent; Amersham Biosciences).

Two-dimensional gel electrophoresis

wt or *crt*$^{-/-}$ cell lysates from D8 EBs were prepared in a buffer containing (in mM): NaCl 150, EDTA 1, Tris 20, Na_3O_4-vanadate 10, and NP-40 1%, pH 8.2. Only the Triton insoluble fraction containing the myofilaments was resuspended in O'Farell's buffer (O'Farrel, 1975) before loading into the electrofocalization capillaries. Unphosphorylated MLC2v was separated from the phosphorylated protein by high-resolution two-dimensional gel electrophoresis (PAGE) as previously described (Hochstrasser et al., 1988; Gravel et al., 1995). Nonlinear immobilized gradient strips (pH 3–10, NL IPG 18 cm; Amersham Biosciences) were used as the first dimension. Hydration of gel strips was performed by sample (100 μg contractile proteins). Focusing started at 500 V for 2 h, and then the voltage was increased to 1,000 V for 2.5 h, to 3,000 V for 1 h, and subsequently it was gradually increased to 5,000 V (at 500 V/15 min) and kept constant overnight (total 24 h). Separation in the second dimension was performed on 9–16% gradient polyacrylamide/piperazine diacrylamide gels (30:0.8 proportion; BioRad Laboratories). The gels (180 × 200 × 1.5 mm) were run in BioRad apparatus at 40 mA per gel, for 3–4 h. Subsequently, proteins were transferred on PVDF membranes (Amersham Biosciences), and Western blot was performed as described above.

We are grateful to Dr. Pierre Travo (the Core Facility of Bitplane European Advanced Imaging Center, CRBM, CNRS UPR1086, member of the European Light Microscopy Initiative), for continuous support and skillful advice on image restoration and analysis, Dr. Frederick Villhardt for his advice on two-dimensional gel electrophoresis, and M. Oliver Plastre for technical help.

This work was supported by grants from the Swiss National Science Foundation (NRP-4046-058712 and 31-55344.98 to M. Jaconi and KH Krause), Fondation de France (2000003470), and Association Française contre les Myopathies (7778 to M. Pucéat), and from Canadian Institutes for Health Research (to M. Michalak). We also gratefully acknowledge the Region Languedoc-Roussillon, INSERM, and Association Française contre le Cancer for their financial support for the acquisition of the light cycler by the Institut Fédératif de Recherche Jean-François Pechère (IFR24) at Montpellier. M. Pucéat is an established investigator of INSERM, and M. Michalak is CIHR Senior Investigator and AHFMR Medical Scientist.

Submitted: 17 April 2002
Revised: 30 May 2002
Accepted: 30 May 2002

References

Aoki, H., J. Sadoshima, and S. Izumo. 2000. Myosin light chain kinase mediates sarcomere organization during cardiac hypertrophy in vitro. *Nat. Med.* 6:183–188.

Bastianutto, C., E. Clementi, F. Codazzi, P. Podini, F. De Giorgi, R. Rizzuto, J. Meldolesi, and T. Pozzan. 1995. Overexpression of calreticulin increases the Ca^{2+} capacity of rapidly exchanging Ca^{2+} stores and reveals aspects of their lumenal microenvironment and function. *J. Cell Biol.* 130:847–855.

Black, B.L., and E.N. Olson. 1998. Transcriptional control of muscle development by myocyte enhancer factor-2 (MEF2) proteins. *Annu. Rev. Cell Dev. Biol.* 14:167–196.

Blaeser, F., N. Ho, R. Prywes, and T.A. Chatila. 2000. Ca^{2+}-dependent gene expression mediated by MEF2 transcription factors. *J. Biol. Chem.* 275:197–209.

Bony, C., S. Roche, U. Shuichi, T. Sasaki, M.A. Crackower, J. Penninger, H. Mano, and M. Puceat. 2001. A specific role of phosphatidylinositol 3-kinase γ. A regulation of autonomic Ca^{2+} oscillations in cardiac cells. *J. Cell Biol.* 152:717–728.

Burns, K., B. Duggan, E.A. Atkinson, K.S. Famulski, M. Nemer, R.C. Bleackley, and M. Michalak. 1994. Modulation of gene expression by calreticulin binding to the glucocorticoid receptor. *Nature.* 367:476–480.

Camacho, P., and J.D. Lechleiter. 1995. Calreticulin inhibits repetitive intracellular Ca^{2+} waves. *Cell.* 82:765–771.

Charron, F., and M. Nemer. 1999. GATA transcription factors and cardiac development. *Semin. Cell Dev. Biol.* 10:85–91.

Chen, J., S.W. Kubalak, S. Minamisawa, R.L. Price, K.D. Becker, R. Hickey, J. Ross, Jr., and K.R. Chien. 1998. Selective requirement of myosin light chain 2v in embryonic heart function. *J. Biol. Chem.* 273:1252–1256.

Clapham, D.E. 1995. Calcium signaling. *Cell.* 80:259–268.

Clement, O., M. Puceat, M.P. Walsh, and G. Vassort. 1992. Protein kinase C enhances myosin light-chain kinase effects on force development and ATPase activity in rat single skinned cardiac cells. *Biochem. J.* 285:311–317.

Colomer, J.M., and A.R. Means. 2000. Chronic elevation of calmodulin in the ventricles of transgenic mice increases the autonomous activity of calmodulin-dependent protein kinase II, which regulates atrial natriuretic factor gene expression. *Mol. Endocrinol.* 14:1125–1136.

Coppolino, M., C. Leung-Hagesteijn, S. Dedhar, and J. Wilkins. 1995. Inducible interaction of integrin alpha 2 beta 1 with calreticulin. Dependence on the activation state of the integrin. *J. Biol. Chem.* 270:23132–23138.

Coppolino, M.G., M.J. Woodside, N. Demaurex, S. Grinstein, R. St-Arnaud, and S. Dedhar. 1997. Calreticulin is essential for integrin-mediated calcium signalling and cell adhesion. *Nature.* 386:843–847.

Corcoran, E.E., and A.R. Means. 2001. Defining Ca^{2+}/calmodulin-dependent protein kinase cascades in transcriptional regulation. *J. Biol. Chem.* 276:2975–2978.

Dedhar, S., P.S. Rennie, M. Shago, C.Y. Hagesteijn, H. Yang, J. Filmus, R.G. Hawley, N. Bruchovsky, H. Cheng, R.J. Matusik, et al. 1994. Inhibition of nuclear hormone receptor activity by calreticulin. *Nature.* 367:480–483.

Doevendans, P.A., R. Bronsaer, P.R. Lozano, S. Kubalak, and M. van Bilsen. 2000. The murine atrial myosin light chain-2 gene: a member of an evolutionarily conserved family of contractile proteins. *Cytogenet. Cell Genet.* 90:248–252.

Durham, P.L., and A.F. Russo. 2000. Differential regulation of mitogen-activated protein kinase-responsive genes by the duration of a calcium signal. *Mol. Endocrinol.* 14:1570–1582.

Durocher, D., C.Y. Chen, A. Ardati, R.J. Schwartz, and M. Nemer. 1996. The atrial natriuretic factor promoter is a downstream target for Nkx-2.5 in the myocardium. *Mol. Cell. Biol.* 16:4648–4655.

Ellgaard, L., and A. Helenius. 2001. ER quality control: towards an understanding at the molecular level. *Curr. Opin. Cell Biol.* 13:431–437.

Fasolato, C., P. Pizzo, and T. Pozzan. 1998. Delayed activation of the store-operated calcium current induced by calreticulin overexpression in RBL-1 cells. *Mol. Biol. Cell.* 9:1513–1522.

Franco, D., M.M. Markman, G.T. Wagenaar, J. Ya, W.H. Lamers, and A.F. Moorman. 1999. Myosin light chain 2a and 2v identifies the embryonic outflow tract myocardium in the developing rodent heart. *Anat. Rec.* 254:135–146.

Frey, N., T.A. McKinsey, and E.N. Olson. 2000. Decoding calcium signals involved in cardiac growth and function. *Nat. Med.* 6:1221–1227.

Friday, B.B., V. Horsley, and G.K. Pavlath. 2000. Calcineurin activity is required for the initiation of skeletal muscle differentiation. *J. Cell Biol.* 149:657–666.

Gravel, P., J.C. Sanchez, C. Walzer, O. Golaz, D.F. Hochstrasser, L.P. Balant, G.J. Hughes, J. Garcia-Sevilla, and J. Guimon. 1995. Human blood platelet protein map established by two-dimensional polyacrylamide gel electrophoresis. *Electrophoresis.* 16:1152–1159.

Gruber, P.J., S.W. Kubalak, and K.R. Chien. 1998. Downregulation of atrial markers during cardiac chamber morphogenesis is irreversible in murine embryos. *Development.* 125:4427–4438.

Han, J., and J.D. Molkentin. 2000. Regulation of MEF2 by p38 MAPK and its implication in cardiomyocyte biology. *Trends Cardiovasc. Med.* 10:19–22.

Harvey, R.P. 1999. Seeking a regulatory roadmap for heart morphogenesis. *Semin. Cell Dev. Biol.* 10:99–107.

Harvey, R.P., and N. Rosental. 1999. Heart Development. Academic Press, San Diego. 530 pp.

Helenius, A., E. Trombetta, D. Hebert, and J. Simons. 1997. Calnexin, calreticulin and the folding of glycoproteins. *Trends Cell Biol.* 7:193–200.

Hochstrasser, D.F., M.G. Harrington, A.C. Hochstrasser, M.J. Miller, and C.R. Merril. 1988. Methods for increasing the resolution of two-dimensional protein electrophoresis. *Anal. Biochem.* 173:424–435.

Jaconi, M., C. Bony, S.M. Richards, A. Terzic, S. Arnaudeau, G. Vassort, and M. Puceat. 2000. Inositol 1,4,5-trisphosphate directs Ca^{2+} flow between mitochondria and the endoplasmic/sarcoplasmic reticulum: a role in regulating cardiac autonomic Ca^{2+} spiking. *Mol. Biol. Cell.* 11:1845–1858.

John, L.M., J.D. Lechleiter, and P. Camacho. 1998. Differential modulation of SERCA2 isoforms by calreticulin. *J. Cell Biol.* 142:963–973.

Krause, K.H., and M. Michalak. 1997. Calreticulin. *Cell.* 88:439–443.

Lin, Q., J. Schwarz, C. Bucana, and E.N. Olson. 1997a. Control of mouse cardiac morphogenesis and myogenesis by transcription factor MEF2C. *Science.* 276:1404–1407.

Lin, Q., D. Srivastava, and E.N. Olson. 1997b. A transcriptional pathway for cardiac development. *Cold Spring Harb. Symp. Quant. Biol.* 62:405–411.

Liu, N., R.E. Fine, E. Simons, and R.J. Johnson. 1994. Decreasing calreticulin expression lowers the Ca^{2+} response to bradykinin and increases sensitivity to ionomycin in NG-108-15 cells. *J. Biol. Chem.* 269:28635–28639.

Liu, Z.P., O. Nakagawa, M. Nakagawa, H. Yanagisawa, R. Passier, J.A. Richardson, D. Srivastava, and E.N. Olson. 2001. Champ, a novel cardiac-specific helicase regulated by mef2c. *Dev. Biol.* 234:497–509.

Lorca, T., F.H. Cruzalegui, D. Fesquet, J.C. Cavadore, J. Mery, A. Means, and M. Doree. 1993. Calmodulin-dependent protein kinase II mediates inactivation of MPF and CSF upon fertilization of *Xenopus* eggs. *Nature.* 366:270–273.

Maltsev, V.A., A.M. Wobus, J. Rohwedel, M. Bader, and J. Hescheler. 1994. Cardiomyocytes differentiated in vitro from embryonic stem cells developmentally express cardiac-specific genes and ionic currents. *Circ. Res.* 75:233–244.

Mery, L., N. Mesaeli, M. Michalak, M. Opas, D.P. Lew, and K.H. Krause. 1996. Overexpression of calreticulin increases intracellular Ca^{2+} storage and decreases store-operated Ca^{2+} influx. *J. Biol. Chem.* 271:9332–9339.

Mesaeli, N., K. Nakamura, E. Zvaritch, P. Dickie, E. Dziak, K.H. Krause, M. Opas, D.H. MacLennan, and M. Michalak. 1999. Calreticulin is essential for cardiac development. *J. Cell Biol.* 144:857–868.

Meyer, N., M. Jaconi, A. Landopoulou, P. Fort, and M. Puceat. 2000. A fluorescent reporter gene as a marker for ventricular specification in ES-derived cardiac cells. *FEBS Lett.* 478:151–158.

Michalak, M., E.F. Corbett, N. Mesaeli, K. Nakamura, and M. Opas. 1999. Calreticulin: one protein, one gene, many functions. *Biochem. J.* 344:281–292.

Mitani, Y., G.R. Dubyak, and F. Ismail-Beigi. 1996. Induction of GLUT-1 mRNA in response to inhibition of oxidative phosphorylation: role of increased $[Ca^{2+}]_i$. *Am. J. Physiol.* 270:C235–C242.

Nakamura, K., M. Robertson, G. Liu, P. Dickie, J.Q. Guo, H.J. Duff, M. Opas, K. Kavanagh, and M. Michalak. 2001a. Complete heart block and sudden death in mice overexpressing calreticulin. *J. Clin. Invest.* 107:1245–1253.

Nakamura, K., A. Zuppini, S. Arnaudeau, J. Lynch, I. Ahsan, R. Krause, S. Papp, H. De Smedt, J.B. Parys, W. Müller-Esterl, et al. 2001b. Functional specialization of calreticulin domains. *J. Biol. Chem.* 154:961–972.

Nguyen-Tran, V.T.B., J. Chen, P. Ruiz-Lozano, and K.R. Chien. 1999. The MLC-2 paradigm for ventricular heart chamber specification, maturation, and morphogenesis. *In* Heart Development. R.P. Harvey and N. Rosental, editors. Academic Press, San Diego. 55–272.

O'Farrel, P.H. 1975. high resolution two-dimensional electrophoresis of proteins. *J. Biol. Chem.* 250:4007–4027.

Olson, E.N., and D. Srivastava. 1996. Molecular pathways controlling heart development. *Science.* 272:671–676.

Olson, E.N., and R. Williams. 2000. Remodeling muscles with calcineurin. *Bioessays.* 22:510–519.

Opas, M., M. Szewczenko-Pawlikowski, G.K. Jass, N. Mesaeli, and M. Michalak. 1996. Calreticulin modulates cell adhesiveness via regulation of vinculin expression. *J. Cell Biol.* 135:1913–1923.

Passier, R., H. Zeng, N. Frey, F.J. Naya, R.L. Nicol, T.A. McKinsey, P. Overbeek, J.A. Richardson, S.R. Grant, and E.N. Olson. 2000. CaM kinase signaling induces cardiac hypertrophy and activates the MEF2 transcription factor in vivo. *J. Clin. Invest.* 105:1395–1406.

Perez-Terzic, C., J. Pyle, M. Jaconi, L. Stehno-Bittel, and D.E. Clapham. 1996. Conformational states of the nuclear pore complex induced by depletion of nuclear Ca^{2+} stores. *Science.* 273:1875–1877.

Pozzan, T., R. Rizzuto, P. Volpe, and J. Meldolesi. 1994. Molecular and cellular physiology of intracellular calcium stores. *Physiol. Rev.* 74:595–636.

Rauch, F., J. Prud'homme, A. Arabian, S. Dedhar, and R. St-Arnaud. 2000. Heart, brain, and body wall defects in mice lacking calreticulin. *Exp. Cell Res.* 256: 105–111.

Sanbe, A., J.G. Fewell, J. Gulick, H. Osinska, J. Lorenz, D.G. Hall, L.A. Murray, T.R. Kimball, S.A. Witt, and J. Robbins. 1999. Abnormal cardiac structure and function in mice expressing nonphosphorylatable cardiac regulatory myosin light chain 2. *J. Biol. Chem.* 274:21085–21094.

Schwartz, R.J., and E.N. Olson. 1999. Building the heart piece by piece: modularity of cis-elements regulating Nkx2-5 transcription. *Development.* 126:4187–4192.

Smith, A.G. 1992. Mouse embryo stem cells: their identification, propagation, and manipulation. *Semin. Cell Biol.* 3:385–399.

Srivastava, D., and E.N. Olson. 2000. A genetic blueprint for cardiac development. *Nature.* 407:221–226.

Sumi, M., K. Kiuchi, T. Ishikawa, A. Ishii, M. Hagiwara, T. Nagatsu, and H. Hidaka. 1991. The newly synthesized selective Ca^{2+}/calmodulin dependent protein kinase II inhibitor KN-93 reduces dopamine contents in PC12h cells. *Biochem. Biophys. Res. Commun.* 181:968–975.

Timmerman, L.A., N.A. Clipstone, S.N. Ho, J.P. Northrop, and G.R. Crabtree. 1996. Rapid shuttling of NF-AT in discrimination of Ca^{2+} signals and immunosuppression. *Nature.* 383:837–840.

Towbin, H., T. Staehelin, and J. Gordon. 1979. Electrophoretic transfer of proteins from polyacrylamide gels to nitrocellulose sheets: procedure and some applications. *Proc. Natl. Acad. Sci. USA.* 76:4350–4354.

Viatchenko-Karpinski, S., B.K. Fleischmann, Q. Liu, H. Sauer, O. Gryshchenko, G.J. Ji, and J. Hescheler. 1999. Intracellular Ca^{2+} oscillations drive spontaneous contractions in cardiomyocytes during early development. *Proc. Natl. Acad. Sci. USA.* 96:8259–8264.

Yang, C.C., O.I. Ornatsky, J.C. McDermott, T.F. Cruz, and C.A. Prody. 1998. Interaction of myocyte enhancer factor 2 (MEF2) with a mitogen-activated protein kinase, ERK5/BMK1. *Nucleic Acids Res.* 26:4771–4777.

Zhang, T., E.N. Johnson, Y. Gu, M.R. Morissette, V.P. Sah, M.S. Gigena, D.D. Belke, W.H. Dillmann, T.B. Rogers, H. Schulman, Jr., J. Ross, and J.H. Brown. 2002. The cardiac-specific nuclear delta(B) isoform of Ca^{2+}/calmodulin-dependent protein kinase II induces hypertrophy and dilated cardiomyopathy associated with increased protein phosphatase 2A activity. *J. Biol. Chem.* 277:1261–1267.

Zou, Y., and K.R. Chien. 1995. EFIA/YB-1 is a component of cardiac HF-1A binding activity and positively regulates transcription of the myosin light-chain 2v gene. *Mol. Cell. Biol.* 15:2972–2982.